Study on Real-time Site Amplification Factor Correction

Quancai Xie[1], Qiang Ma[1], Jingfa Zhang[2], Haiying Yu[1]

[1]Key Laboratory of Earthquake Engineering and Engineering Vibration, Institute of Engineering Mechanics, China Earthquake Administration, Harbin, 150080, China

[2]Institute of Crustal Dynamics, China Earthquake Administration, Beijing 100085, China

Correspondence to: Quancai Xie (xiequancai@iem.ac.cn)

Abstract. The site amplification factor was usually considered as scalar values, such as amplification of peak ground acceleration or peak ground velocity, increments of seismic intensity in the earthquake early warning system or seismic intensity repaid report system. This paper focus on evaluation of infinite impulse recursive filter method that could produce frequency-dependent site amplification and compare the performance of the scalar value method with the infinite impulse recursive filter method. A large amount of strong motion data of IBRH10 and IBRH19 of Kiban Kyoshin network (Kik-net) triggered in more than one thousand earthquakes from 2004 to 2012 were selected carefully and used to get the relative site amplification, then we model the relative site amplification factor by casual filter. Then we make simulation from borehole to surface and also simulation from front-detection station to far-field station. Compare different simulation cases, it can easily be found that this method could produce different amplification factor for different earthquakes and could reflect the frequency-dependent of site amplification. Through these simulation between two stations, we can find that the frequency-dependent correction for site amplification show better performance than the ARV method and station correction method. It also shows better performance than the average level and the highest level of Japan Meteorological Agency (JMA) earthquake early warning system in ground motion prediction. This method pays attention to the amplitude and ignore the phase characteristic, this problem may be improved by the seismic interferometry method. Although there are some problems needed to be considered and solved carefully, frequency-dependent correction for site amplification in the time domain highly improve the accuracy of predicting ground motion real-timely.

1 Introduction

In recent decades, real-time strong ground motion prediction has become an important part of earthquake early warning systems. In the world, there are many countries deployed operational earthquake early warning systems like Mexico (Espinosa-Aranda et al. 1995; Espinosa-Aranda et al. 2009), Japan (Kamigaichi et al. 2004; Hoshiba 2008;Nakamura et al. 2009), Taiwan (Wu et al. 2002; Hsiao et al. 2009), Turkey (Erdik et al. 2003; Alcik et al. 2009), and Romania (Wenzel et al. 1999; Ionescu et al. 2007) Also there are many some earthquake early warning system under developing and testing like the Unites States (Allen et al .2003; Allen et al. 2009; Bose et al. 2009;), Italy (Zollo et al. 2006; Zollo et al. 2009), and China (Peng et al. 2011). Usually, the earthquake early warnings systems can be categorized as offsite (also known as regional EEW) and onsite warnings. The offsite warning utilizes a few seconds of seismogram observed at the first station, and then estimate the source

parameter, such as magnitude, epicentre distance or others. Then according to the parameter estimated, a warning can be manually or automatically issued based on some rules made before an earthquake occurs. Hoshiba et al., 2008 mentioned that the Japan earthquake early warning system has been operational nationwide since October, 2007 by Japan Meteorological Agency. Approximately 1,100 stations from JMA network and the high sensitivity seismograph network (Hi-net) were used to determine the hypocenter of Japan Meteorological Agency earthquake early warning system. In order to disseminate the warning quickly, hypocentre estimation should be done just after the first detection of the P phase at a single station. In order to ensure the reliability of the estimation, the B-Delta Method (Odaka et al., 2003) and Network Method (Horiuchi et al., 2005; Horiuchi et al., 2009) are used in combination. Usually, the current Japan Meteorological Agency earthquake early warning system works well. But after the main shock of the 2011 great Tohoku Earthquake, the earthquake early warning system did not work well due to high aftershocks activity and high background noise, as well as power failure and wiring disconnections (Hoshiba, 2011). Earthquakes that occurred nearby simultaneously in different locations also made the system provide false information. The site amplification factor was usually considered as scalar values, such as amplification of peak ground acceleration or peak ground velocity, increments of seismic intensity, in the conventional earthquake early warning system. There are some research papers on how to improve the site amplification factor for considering more accuracy calculating Japan Meteorological Agency seismic intensity of Japan earthquake early warning system (e.g., Iwakiri et al., 2011). Among them we chose the new idea proposed by Hoshiba (2013) and used it to design casual Filter for modelling the site amplification factor of Kik-net stations .We focus on full evaluate the performance of this method by selecting large amount of Kik-net data triggered in more than one thousand earthquakes, then we make simulation from borehole to surface and also simulation from front-detection station to far-field station. Then compare the statistical simulation result with other methods considering the accuracy of the seismic intensity prediction and clarify the advantages and some problem need to be considered when utilizing it to the earthquake early warning system.

2 Data

The hypocentre parameters including origin time, location of hypocentre, and magnitude were obtained from the JMA seismic catalogue. The strong motion data were downloaded from the website (http://www.kyoshin.bosai.go.jp/).The advantage of this network is that all stations have a borehole of 100 m or more in depth, with acceleroagraphs installed both on the ground surface and at the bottom of boreholes. The site information measured in the boreholes includes soil type along with P and S wave velocity profiles. The sampling frequency is 200Hz for the records before November 2007 and is 100Hz thereafter. In this analysis, we use records observed at 2 stations. One of them with site code IBRH10 has been in operation since September 1, 2000 and the other with site code IBRH19 since May 15, 2004, respectively. Until Decmber.31, 2012, IBRH10 and IBRH19 recorded 1119 and 910 events respectively. We selected 673 strong ground motion records which was recorded at the surface and borehole sensor when both of these two stations were triggered by an earthquake. The inner distance between IBRH10 and IBRH19 is 14.6 km. We selected strong motion data with hypocentre distance larger than at least three times of the inner

distance. The number of earthquakes is up to 553 and the range of magnitude was between 3.3 and 9. The recording time spans from May 16, 2004 to December 31, 2012. Excluding the earthquake which occurred in the sea area, the number of earthquakes ranging from Magnitude 3.3 to Magnitude 7 adds up to 208 (Figure 1). There exists 20 meter soft sediment at station IBRH10.The layer of appears at the depth of 518m.The IBRH19 is almost a completely rock site station. The site profiles can be downloaded from the Kik-net website.

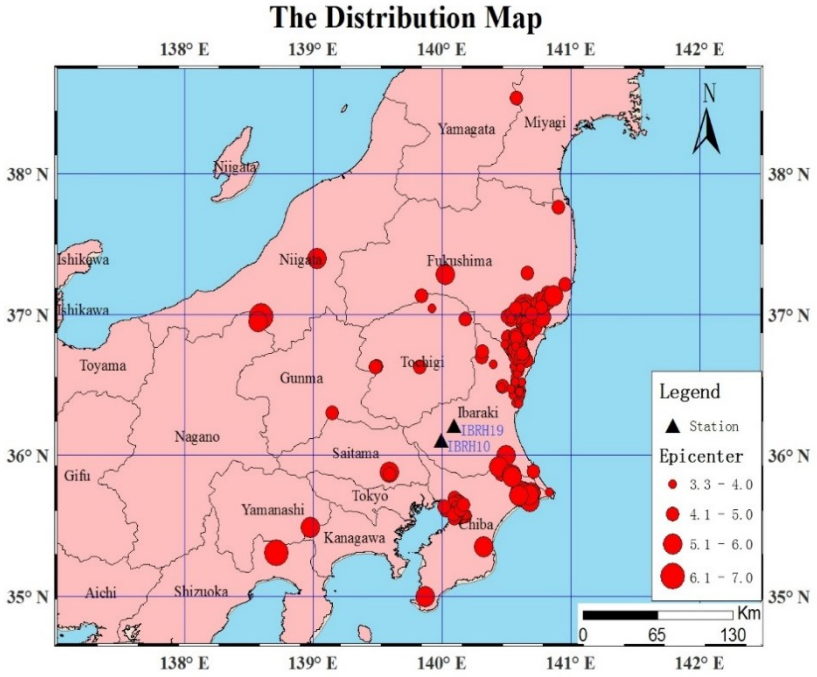

Figure 1. The station and epicentre distribution map used for this research.

3 Theory and Methodology

Source parameters including hypocentre location and magnitude are determined within a few seconds after an earthquake occurrence. Then the ground motions are estimated based on these parameters. While the EEW using a few parameters, parameter uncertainty leads to another error in the ground motion prediction. A new method was proposed by Hoshiba (2013). The method predicts ground motion using ground motions observed at front stations in the direction of incoming waves. The idea of this method were shown in Figure 2. In this method, the observed information is sent directly forward to the target point. The core idea of this method is that the frequency-dependent site amplification factor can be reproduced by a casual recursive filter based on historical relative spectrum ratio between two stations. In the method the far-field simulated waveform can be obtained by real-time filtering of the observed waveform recorded in the front detection station.

Seismic ground motions are often modelled by convolution of source, propagation and site amplification factors. Site amplification factor plays important role in determine seismic wave amplitude except for propagation effect and source effect. Usually, the site amplification factor was evaluated in frequency domain. However, for earthquake early warning systems it is not suitable as this procedure needs some length windowed waveform for FFT in frequency domain. In many previous studies, site amplification factors are estimated using following equation. (e.g., Iwata and Irikura (1988))

$$O_{kl}(f) = S_k(f)G_l(f)T_{kl}(f) \quad (1)$$

Where f is frequency in Hz, $O_{kl}(f)$, $S_k(f)$, $G_l(f)$, and$T_{kl}(f)$represent the observed seismic spectrum from event *k* at site *l*, the source spectrum characterizing the event *k*, the site amplification factor at site *l*, and the propagation factor between event *k* and site *l* respectively, and *f* is the frequency of the seismic waves.

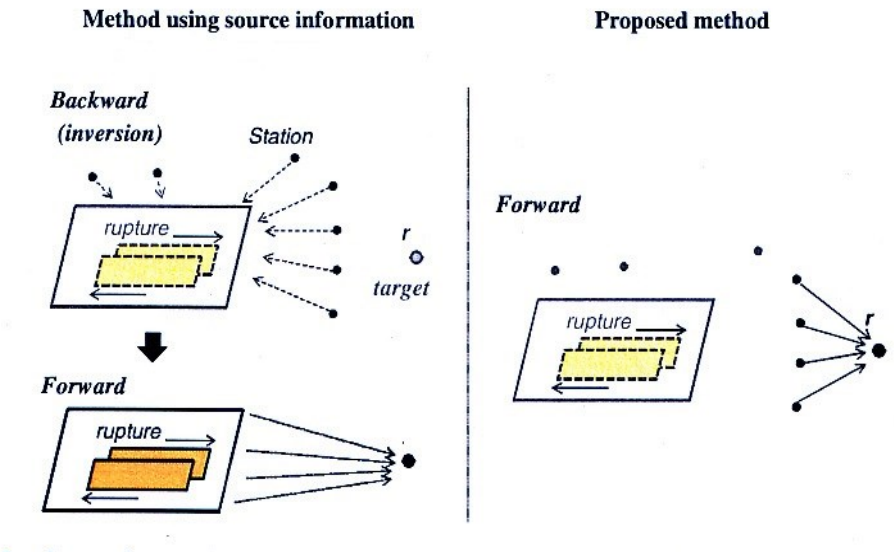

Figure 2. Comparison of the method proposed by Hoshiba with the network method. (Modified after Hoshiba, 2013)

The frequency-dependent relative site amplification factors are assumed to be modelled by a following linear system of first- and second –order filters,

$$\mathrm{F(s)} = G_0 \prod_{n=1}^{N} \left(\frac{\omega_{2n}}{\omega_{1n}}\right) \cdot \frac{s+\omega_{1n}}{s+\omega_{2n}} \cdot \prod_{m=1}^{M} \left(\frac{\omega_{2m}}{\omega_{1m}}\right)^2 \cdot \frac{s^2+2h_{1m}\omega_{1m}+\omega_{1m}^2}{s^2+2h_{1m}\omega_{1m}+\omega_{2m}^2} \quad (2)$$

where *N* and *M* stand for the numbers of the first and second-order filters, respectively, and $\mathrm{s} = \mathrm{i}\omega$. Here ω are angular frequencies and *h* are damping factors that characterize the frequency dependence, respectively.$s^2 + 2h\omega + \omega_m^2$ represents a damping oscillation (Hoshiba, 2013).G_0,ω_{1n}, ω_{2n} , ω_{1m} , ω_{2m} are estimated for given values of *N* and *M* by using the least-

squares method in logarithmic scales. We focus on the amplitude characteristics, ignoring phase characteristics. The bilinear transform (also known as Tustin's method) is introduced as

$$s = \frac{2}{\Delta T} \cdot \frac{1-Z^{-1}}{1+Z^{-1}} \quad (3)$$

Which is used in digital signal processing and discrete-time control theory to transform continuous-time system representations to discrete-time. Then the pre-warping equation

$$\omega \rightarrow \frac{2}{\Delta T} \tan\left(\frac{\omega \Delta T}{2}\right) \quad (4)$$

is applied to ω_{1n}, ω_{2n} , ω_{1m} , ω_{2m} , Then the transfer function$F(z)$ is obtained, whereΔT is the sampling interval of the digital waveforms and $z = \exp(s\Delta T)$. Eq. (3) and Eq. (4) are the necessary procedures to obtain the coefficients of a causal recursive filter for real time processing.

4 Result analysis

4.1 Spectral Ratios

We use the strong motion data recorded by IBRH10 and IBRH19 during these 208 earthquakes. The spectral ratio results obtained are shown in Figure 3(a) to Figure 6(f). Parzen window of 0.3Hz bandwidth was used to smooth the spectra. The spectral ratios of EW component and NS component of IBRH10 have similar tendencies. It is approximately 30 at around 1.3~1.5Hz; whereas it is less than 2 at around 20HZ (Figure 3(a) and (b)).The spectral ratio of UD component of IBRH10 is approximately 10 at around 2~3Hz whereas it is less than 2 at around 25HZ (Figure 3(c)).The Spectral ratios of EW component and NS component of IBRH19 also have similar tendencies. It is approximately 6 at around 5Hz and 4 at 13Hz, respectively, whereas it is less than 2 at less than 2 Hz (Figure 4(a) and (b)). The spectral ratio of UD component of IBRH19 is approximately 5 at 5Hz and 4 at 25Hz, respectively, whereas it is less than 2 at around 3HZ (Figure 4(c)). The spectral ratio of the borehole component of IBRH10 to IBRH19 is almost flat, as this ratio is calculated from bedrock to bedrock. The maximum site amplification is 2.5 at about 20Hz, and the spectral ratio is nearly 1 at the rest of the frequency (Figure 5(a), (c) and (e)). The spectral ratios of the EW component and NS component of IBRH10 surface to IBRH19 surface are approximately 20 at 1Hz to 2Hz, whereas it is less than 1 from 17Hz to 30 Hz (Figure 5(b) and (d)). The spectral ratio of the UD component of IBRH10 surface to IBRH19 surface is approximately 10 at 1.5Hz, whereas it is less than 1 from 22Hz to30 Hz (Figure 5(f)).

(a)

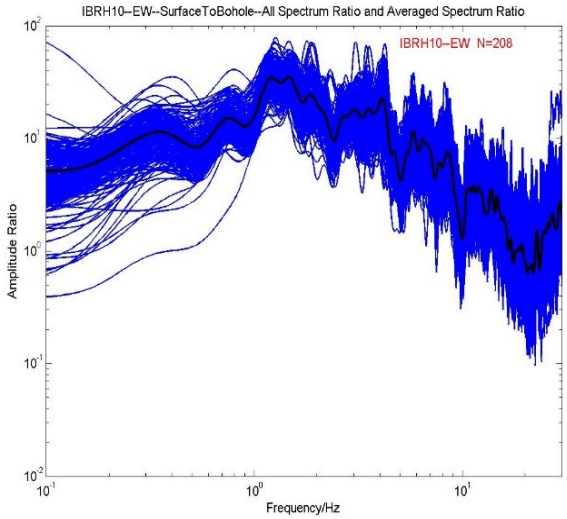

(b)

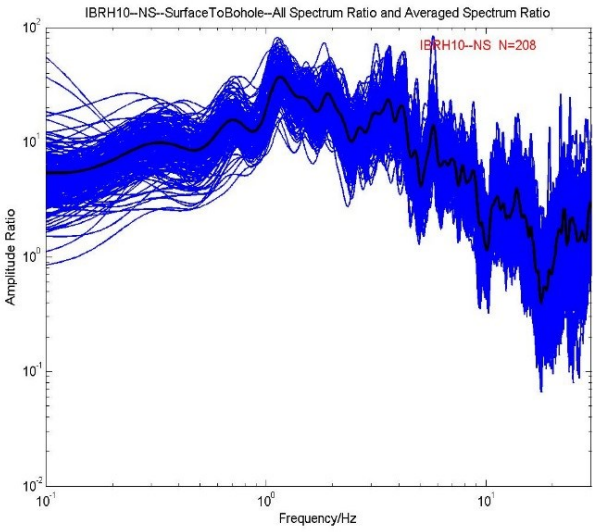

(c)

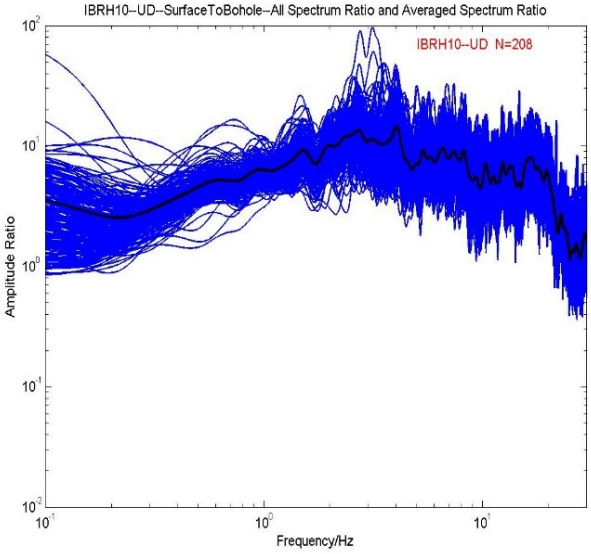

Figure 3. Surface to Borehole Spectral Ratios at IBRH10: (a) EW2/EW1, (b) NS2/NS1, (c) UD2/UD1. The blue lines stand for the spectra ratio for every earthquake event and the black one stands for the average spectra ratio for all the events.

(a)

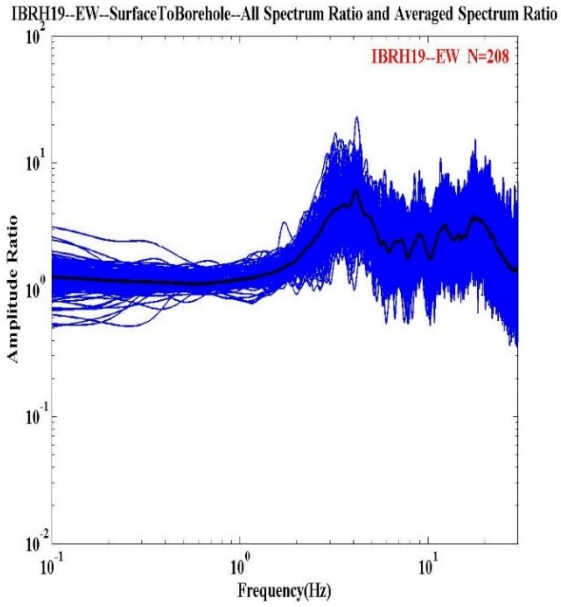

(b)

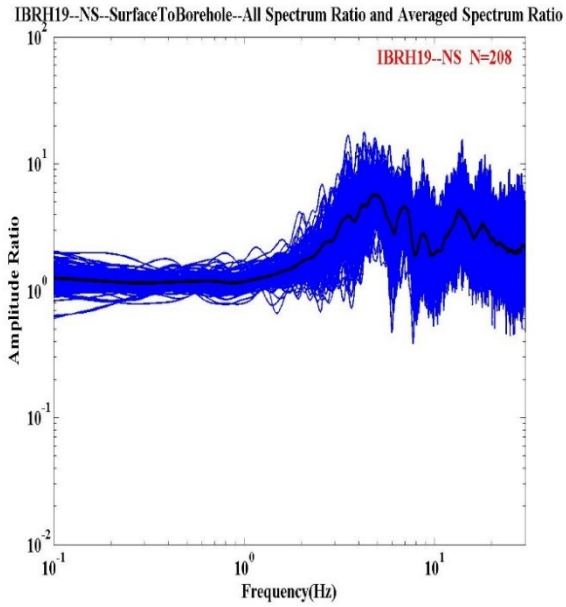

(c)

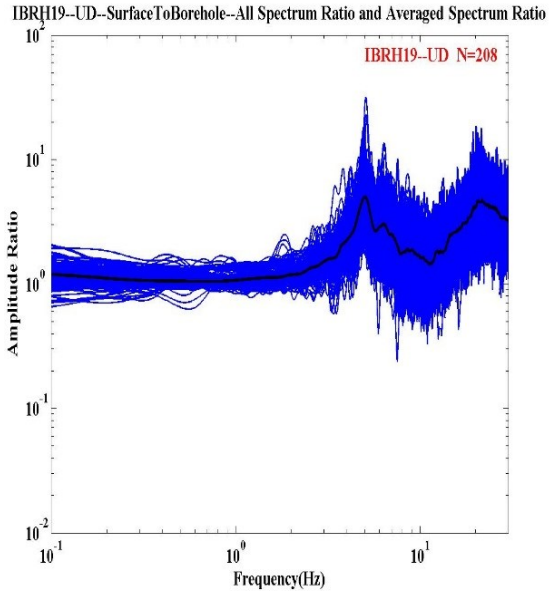

Figure 4. Surface to Borehole Spectral Ratios at IBRH19: (a) EW2/EW1, (b) NS2/NS1, (c) UD2/UD1.The blue lines stand for the spectra ratio for every earthquake event and the black one stands the average spectra ratio for all the events.

(a)

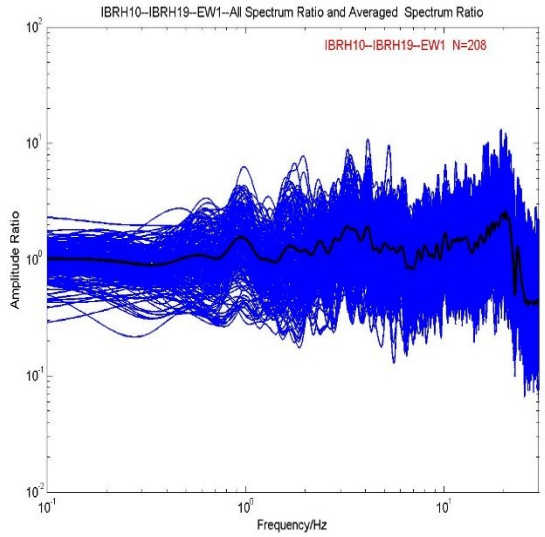

(b)

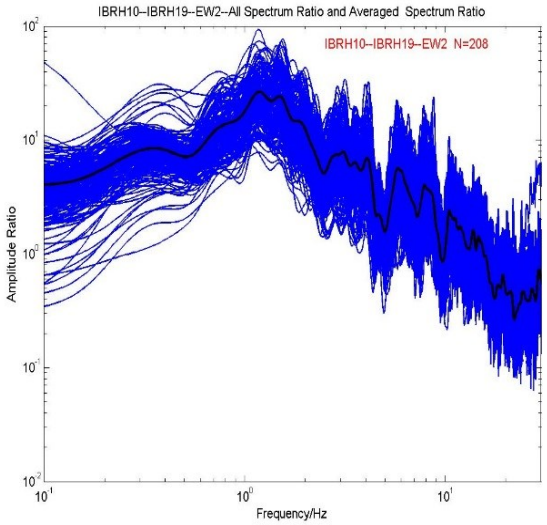

(c)

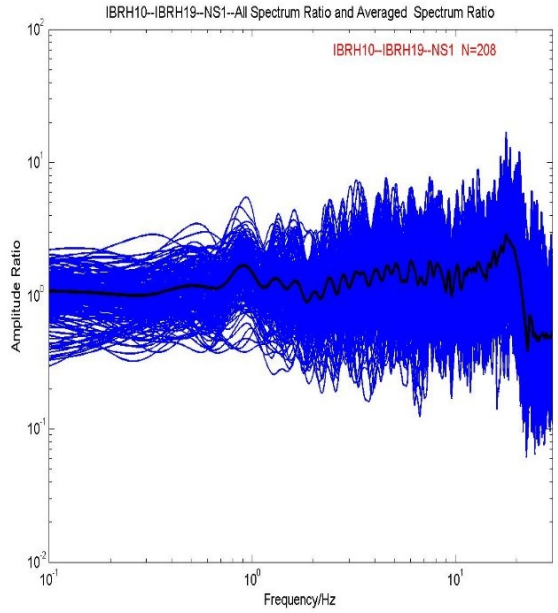

(d)

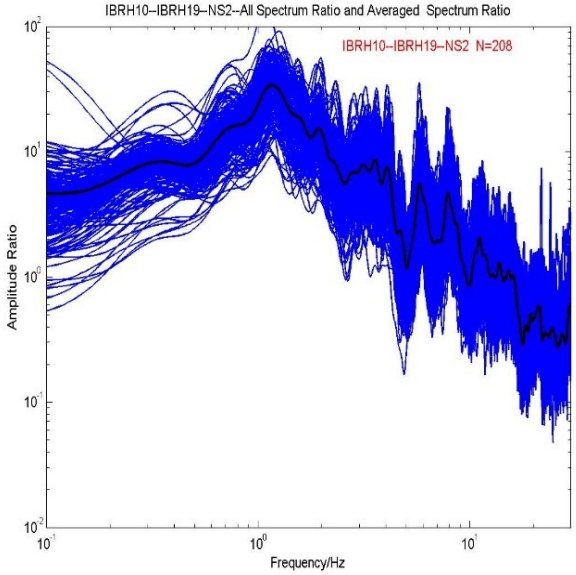

Figture 5. spectral ratios of IBRH10 to IBRH19 for: (a) EW1, (b) EW2, (c) NS1, (d) NS2.The blue lines stan for the spectra ratio for every earthquake event and the black one stands the average spectra ratio for all th events. (to be continued)

(e)

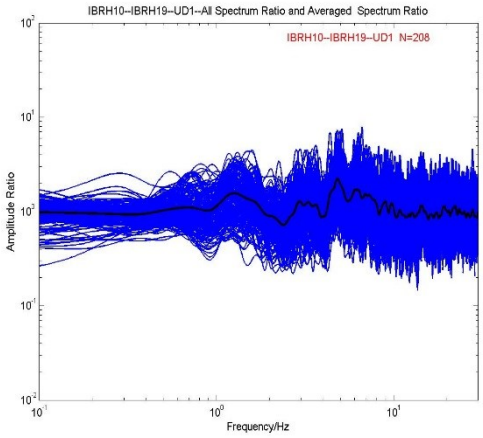

(f)

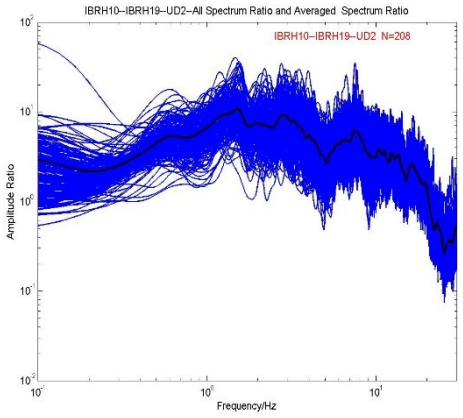

Figture 5. spectral ratios of IBRH10 to IBRH19 for: (e) UD1, (f) UD2. The blue lines stand for the spectra ratio for every for every earthquake event and the black one stands the average spectra ratio for all the events (Continued)

4.2 Simulation from borehole to surface

Firstly, we make the simulation from borehole to surface, although it is not useful for earthquake early warning system. But it could be used to make full evaluation of this method. We use the strong motion data recorded by IBR10 borehole sensor to simulate the surface station acceleration waveforms and spectrum. Figure 6(a) to Figure 6(d) shows the simulation results for the M4.5 earthquake which occurred on November 21, 2009. The information about the site amplification factors and the increment of seismic intensity are summarized in in Table1.In the table, the abbreviation for Amplification is Amp. The abbreviation for Observation is Obs. The abbreviation for Simulation is Sim. The abbreviation for Component is comp. The abbreviation for Residual is Res. The abbreviation for Borehole is Boh. The abbreviation for Surface is Suf.

Table 1 Information for M4.5 earthquake (IBRH100911211539)

	PGA (gal)			PGA Amp.		I_{jma}					
	Boh.	Suf.		Amp. (Suf./Boh.)		Bore.	Surf.		Difference (Suf.-Boh.)		Res. (Sim.-obs.)
Comp.	Obs.	Obs.	Sim.	Obs.	Sim.	Obs.	Obs.	Sim.	Obs	Sim.	
NS	1.9	13.2	16.8	6.9	8.8						
EW	1.4	7.5	12.1	5.4	8.6	1.1	3.1	3.3	2.0	2.2	0.2
UD	0.7	4.1	5.6	5.9	8.3						

Figure 7(a) to Figure 7(d) show the simulation results for the M4.6 earthquake which occurred on December 7, 2012. The information about the site amplification factors and the increment of seismic intensity are summarized in Table 2.

Table 2 Information for M4.6 earthquake (IBRH101212070532)

	PGA (gal)			PGA Amp.		I_{jma}					
	Boh.	Suf.		Amp. (Suf./Boh.)		Boh.	Surf.		Difference (Suf.-Boh.)		Res. (Sim.-obs.)
Comp.	Obs.	Obs.	Sim.	Obs.	Sim.	Obs.	Obs.	Sim.	Obs	Sim.	
NS	0.7	2.7	3.6	3.9	5.1	0.0	1.2	1.3	1.2	1.3	0.1
EW	0.6	3.3	4.0	5.5	6.7						
UD	0.4	2.9	2.4	7.3	6						

For these two examples, compared the simulated acceleration and spectrum with the observed acceleration and spectrum of the surface records, the result simulated well. The different amplifications of maximum acceleration between Table 1 and Table 2 reflect the differences of the frequency contents of the incident waveforms that cannot be reproduced by a scalar site amplification factor (e.g., amplification of peak ground acceleration or peak ground velocity, or increment of seismic intensity).

The seismic intensity is calculated according to the method described in the paper (Yamazaki et al. 1998). Figure 8 shows the seismic intensity residuals. The average seismic intensity residuals of these 208 earthquakes is 0.139. The standard deviation of the difference is 0.254. 98.6% of the seismic intensity residuals is less than 0.5. 100% of the seismic intensity residuals is less than 1. As the minimum resolution for the seismic calculation is 0.1 degree, It is reasonable that we consider these simulations show good performance.

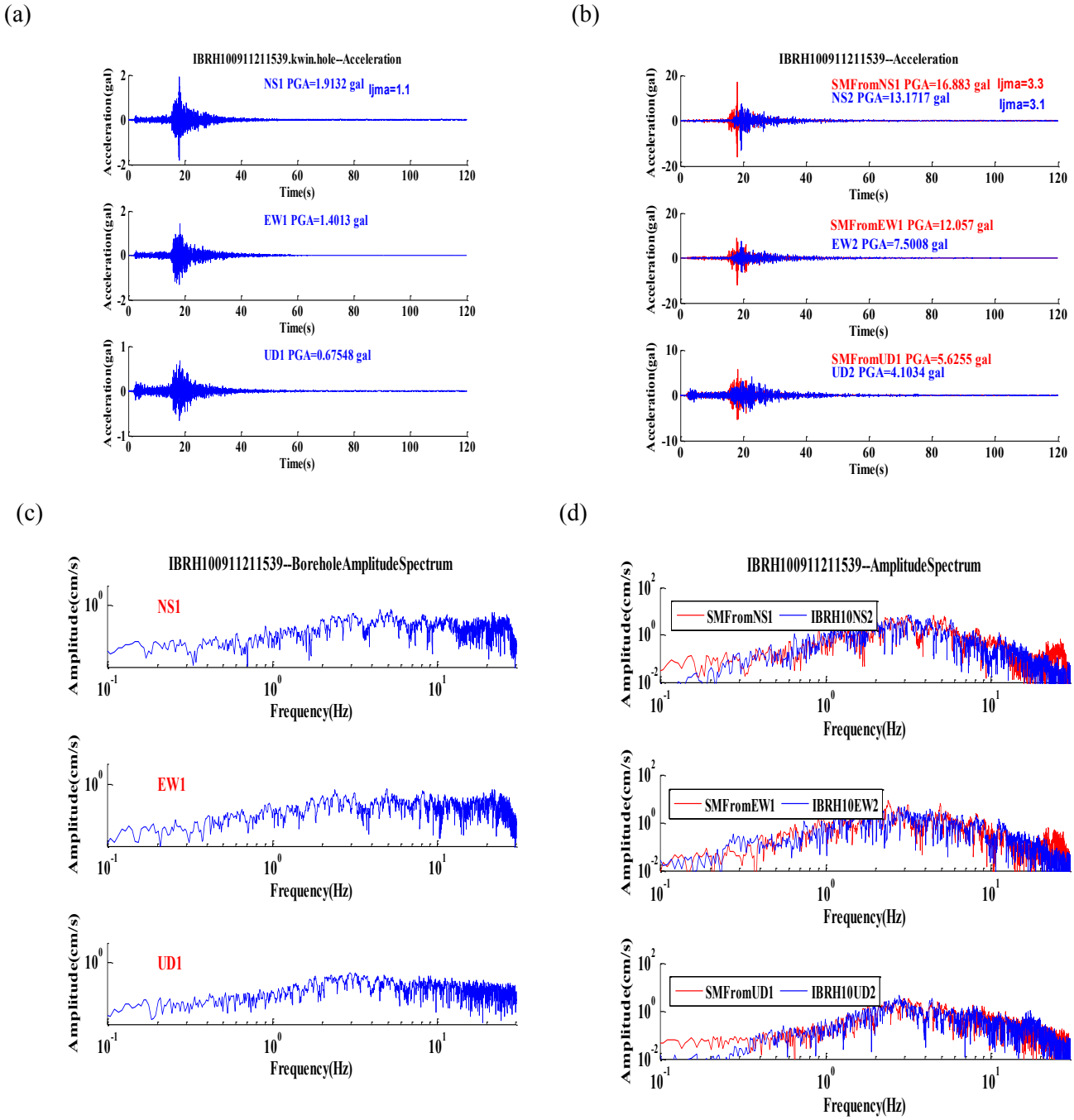

Figure 6. An example of the results of simulation for IBRH100911211539: (a) the observed accerlation at the borehole, (b) the observed surface acceleration waveform (blue) compared with the simulated one (red), (c) the spectra of the observed surface record, (d) the spectra of the observed surface record (blue) compared with the simulated one (red).

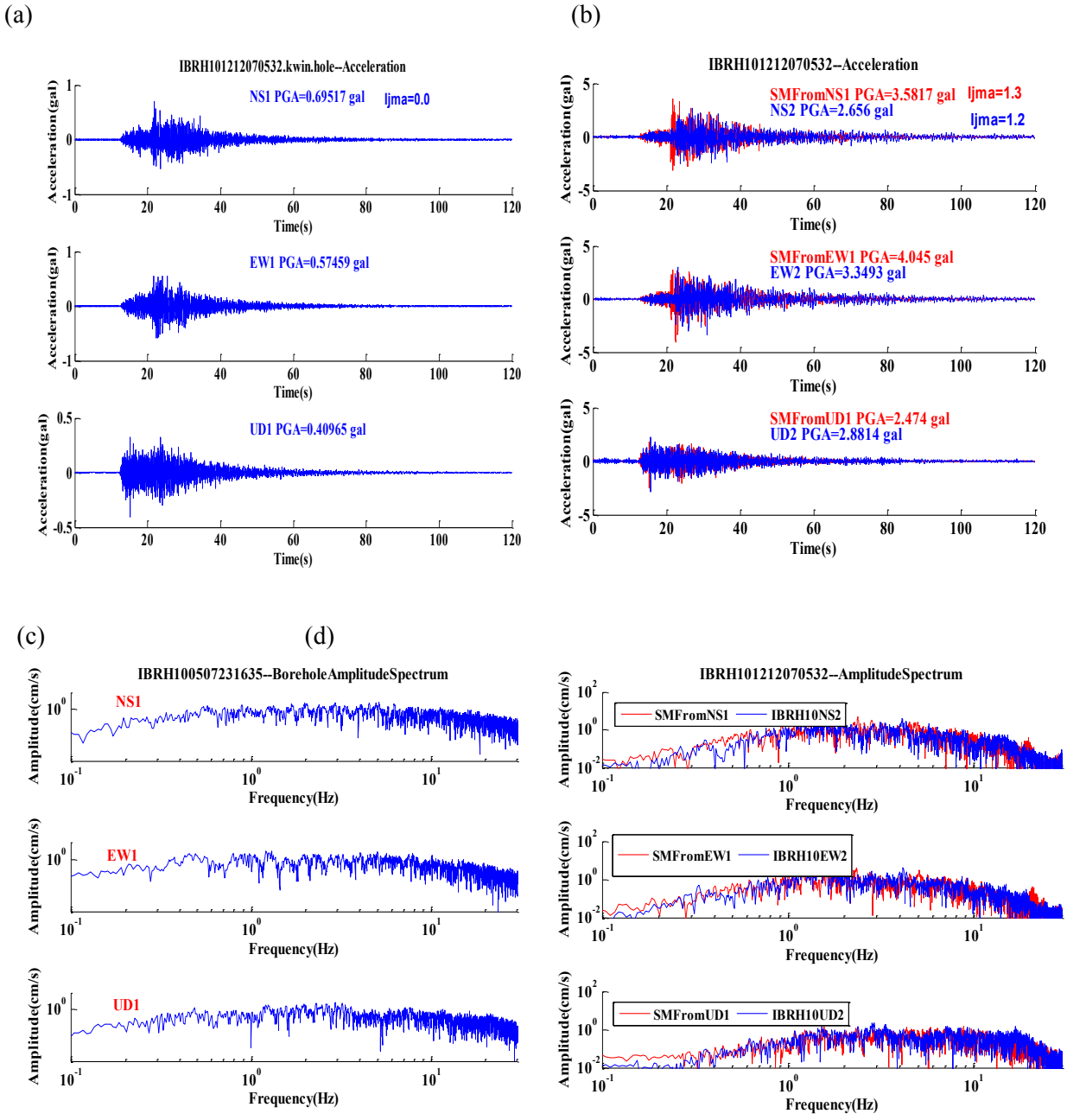

Figure 7. An example of the results of simulation for IBRH101212070532: (a) the observed accerlation at the borehole, (b) the observed surface acceleration waveform (blue) compared with the simulated one (red), (c) the spectra of the observed surface record, (d) the spectra of the observed surface record (blue) compared with the simulated one (red).

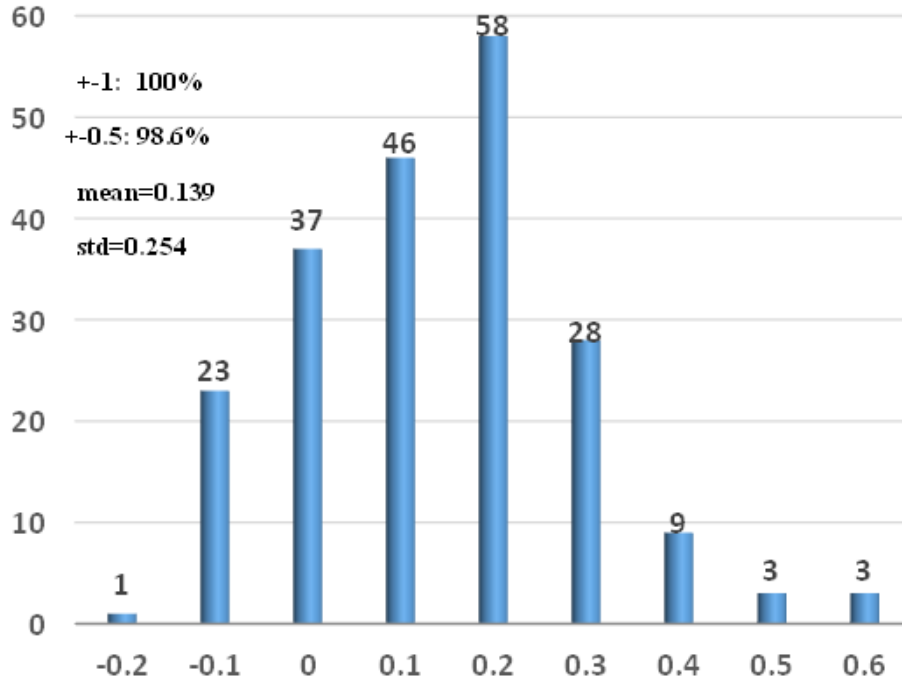

Figure 8. The seismic intensity residuals between observed data and simulated data.

4.3 Simulation Between Front-detection Station and Far-flied Station

Then, Using the surface strong motion data of IBRH19,we get simulated waveforms for IBRH10. Figure 9(a) through Figure 9(d) show the simulation results for the M5.2 earthquake which occurred on Feb. 19, 2012. The information about site amplification factors and the increment of seismic intensity are summarized in Table 3.

Table 3 Information for M5.2 earthquake (IBRH10 & IBRH19 for 201202191454)

	PGA(gal)			PGA Amp.		I_{jma}			
	IBRH19	IBRH10		Amp. (IBRH10/IBRH19)		IBRH19	IBRH10		Res. (Obs.-Sim.)
Comp.	Obs.	Obs.	Sim.	Obs.	Sim.	Obs.	Obs.	Sim.	
NS	17.7	50.9	69.7	2.8	3.9	2.2	3.5	3.7	0.2
EW	13.6	45.7	53.2	3.3	3.9				
UD	11.2	23.7	38.9	2.1	3.5				

The simulation results for the M5.1 earthquake occurred on April 14,2011 is shown in Figure 10(a) to Figure 10(d) . The comparison information about the site amplification factors and the increment of seismic intensity are summarized in Table 4.

Table 4 Information for M5.1 earthquake (IBRH10 & IBRH19 for 201104140735)

	PGA(gal)			PGA Amp.		I_{jma}			
	IBRH19	IBRH10		Amp. (IBRH10/IBRH19)		IBRH19	IBRH10		Res. (Obs.-Sim.)
Comp.	Obs.	Obs.	Sim.	Obs.	Sim.	Obs.	Obs.	Sim.	
NS	7.1	25.4	16.7	3.6	2.4	1.3	2.7	2.7	0
EW	7.1	18.1	17.6	2.5	2.5				
UD	4.3	14.6	16.7	3.4	3.9				

Compared the observed the surface record acceleration and spectrum with the simulated acceleration and spectrum, it shows that the simulation result is well. The acceleration amplification factor for the he M5.2 earthquake which occurred on Feb. 19, 2012 is 3.9,3.9,3.5 respectively, while the acceleration amplification factor for the he M5.1 earthquake which occurred on April 14,2011is 2.4,2.5,3.9 respectively. Comparing the simulation results for these two earthquakes, the different amplifications of acceleration between Table 3 and Table 4 shows the different frequent contents of the waveforms that cannot be reproduced by a scalar site amplification method.

Although most of the simulation result shows good performance, there exists the case that the simulation did not work well. For example, Figure 11(a) to Figure 11(d) shows the simulation results for the M5.3 earthquake occurred on March 16, 2011. The information about the site amplification factors and the increment of seismic intensity are summarized in Table 5.Compared the observed acceleration and spectra with simulated acceleration and spectra, it indicates that the simulation did not work well for the M5.3 earthquake occurred on March 16, 2011.

Table 5 Information for M5.3 earthquake (IBRH10 & IBRH19 for 201103162239)

	PGA(gal)			PGA Amp.		I_{jma}			
	IBRH19	IBRH10		Amp. (IBRH10/IBRH19)		IBRH19	IBRH10		Res. (Obs.-Sim.)
Comp.	Obs.	Obs.	Sim.	Obs.	Sim.	Obs.	Obs.	Sim.	
NS	6.1	10.7	34.9	1.8	5.7	1.5	2.7	3.8	1.1
EW	5.0	12.6	36.1	2.5	7.2				
UD	3.9	6.2	22.2	1.6	5.7				

The seismic intensity is calculated according to the method described in the paper(Yamazaki et al. 1998). Figure 12 shows the seismic intensity residual. The average seismic intensity residual is 0.35 for all our data set. The standard deviation of seismic intensity residual is 0.36. 69.7% of the seismic intensity residual is less than 0.5. 98.1% of the seismic intensity residual is less than 1. Japan Meteorological Agency used ARV method (amplitude ratio of peak ground velocity at the ground surface relative to the engineering bedrock of averaged S-wave velocity 700 m/s) based on topographic data. Iwakiri et al. 2011 proposed the station correction method. The station correction method based on site amplifications obtained empirically from observed seismic intensity data.

We compared the performance of this method with the ARV method and station correction method. For the ARV method and station correction method, The seismic intensity residual within +-0.5 is 55% and 59%, respectively. The seismic intensity residual within +-1 is 84% and 93% respectively for ARV method and station correction method. The comparison result between different methods are shown in Table 6. The statistical 1 degree seismic intensity error of the current JMA EEW system (JMA,2018) was shown in figure 13. The average 1 degree seismic intensity error is 74.74% for all the eleven years data. The best case is 93.7% in 2017,the worst case is 34.6% in 2010.From the analysis mentioned above, we can conclude that this method could improve the accuracy of the seismic intensity estimation. It highly improve the accuracy of predicting ground motion real-timely. It could be used to the earthquake early warning system.

Table 6. The comparison result

Method	mean residual	standard deviation	+-0.5	+-1.0
ARV(Iwakiri et al. 2011),	0.25	0.63	55%	84%
Station Correction (Iwakiri et al. 2011),	0.19	0.55	59%	93%
This paper	0.35	0.36	69.7%	98.1%

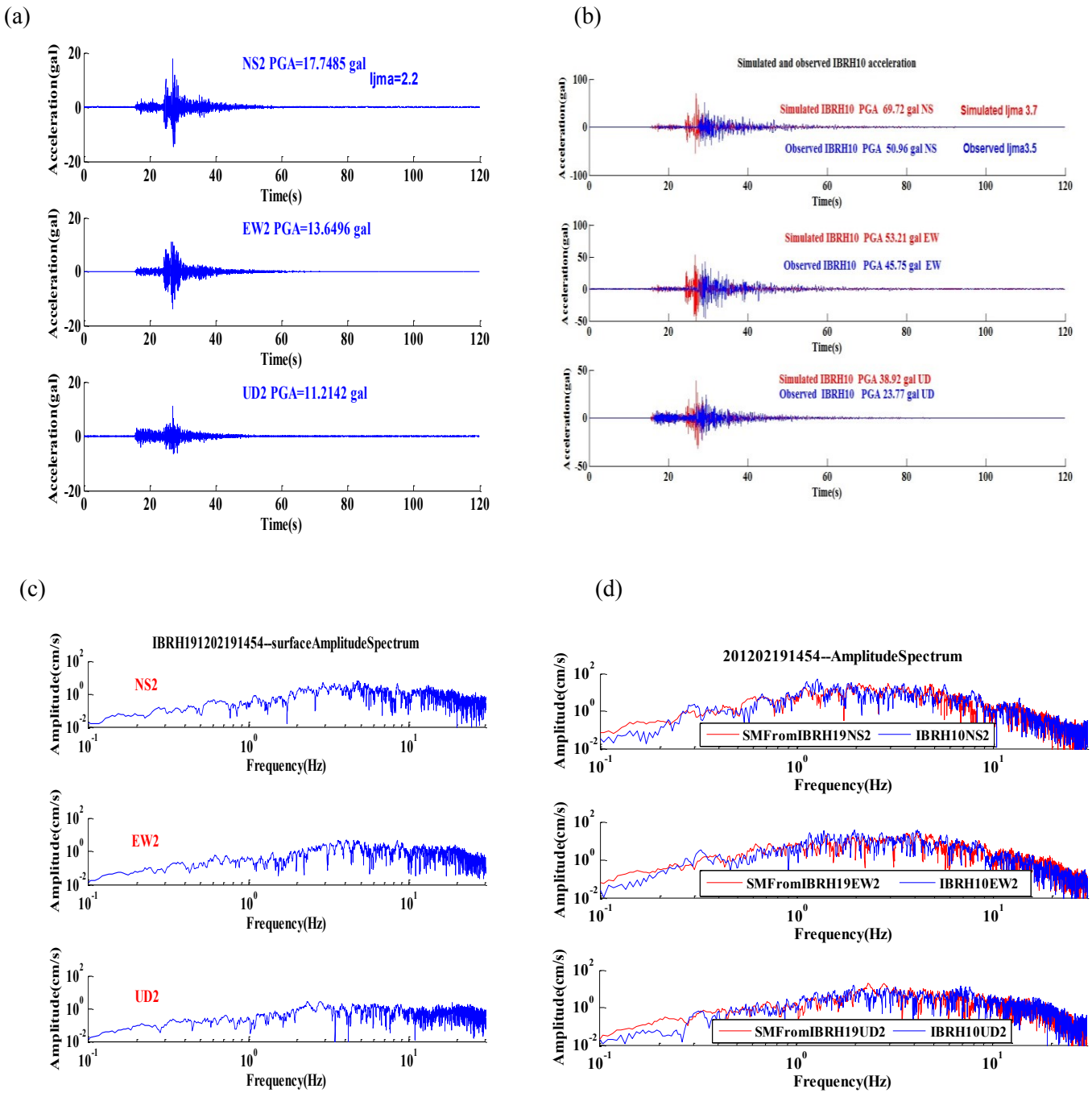

Figure 9. An example of simulation from IBRH19 (surface) to IBRH10 (surface) for the earthquake 201202191454: (a)the observed surface acceleration forIBRH19, (b) the observed surface acceleration waveform (blue) compared with the simulated one (red), (c) the spectral of observed surface record for IBRH19, (d)the observed spectra of surface record at IBRH10 (blue) compared with the simulated one (red)

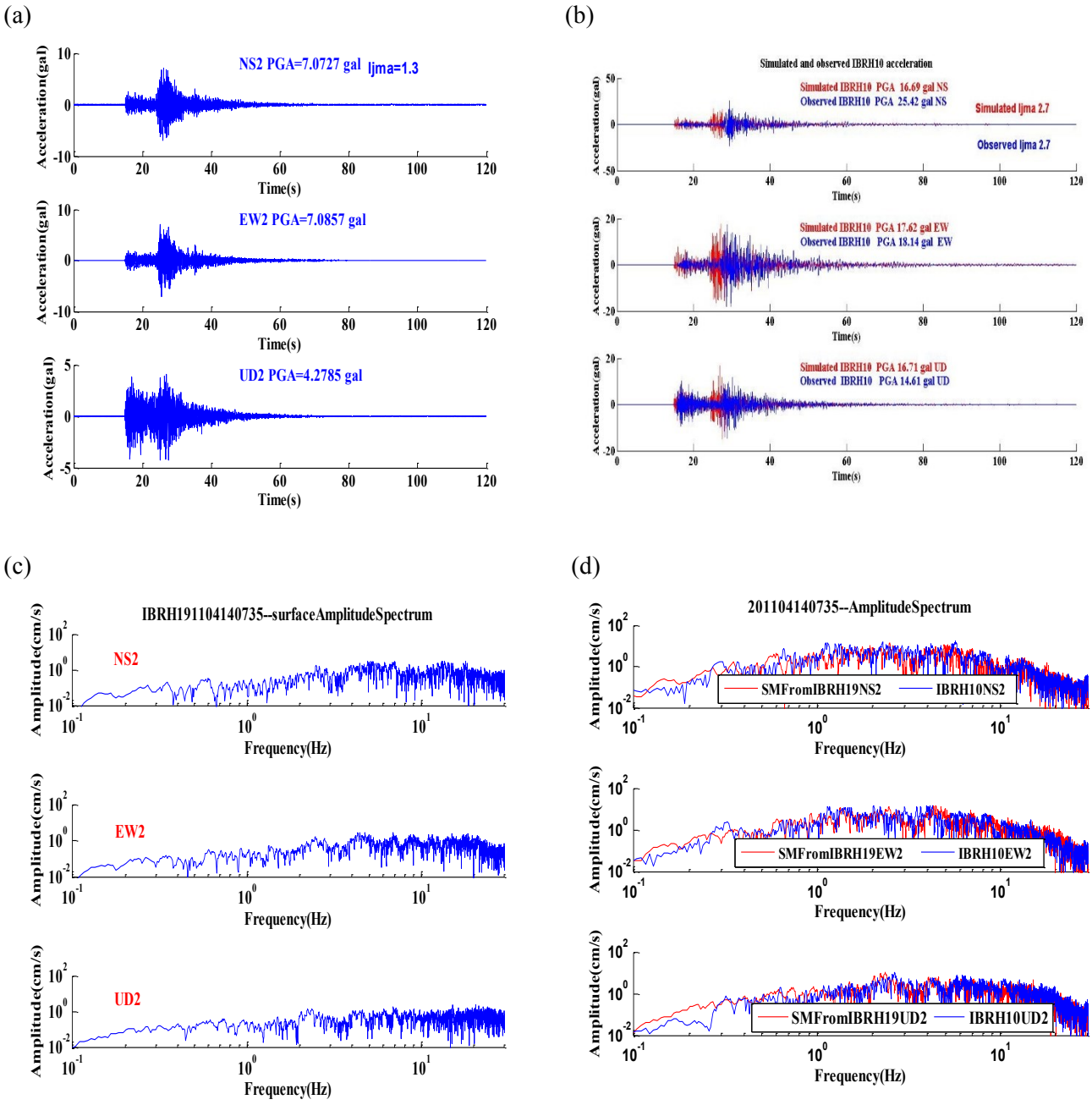

Figure 10. An example of simulation from IBRH19 (surface) to IBRH10 (surface) for the earthquake 201104140735: (a) the observed surface acceleration forIBRH19, (b) the observed surface acceleration waveform (blue) compared with the simulated one (red), (c) the spectral of observed surface record for IBRH19, (d) the observed spectra of surface record at IBRH10 (blue) compared with the simulated one (red)

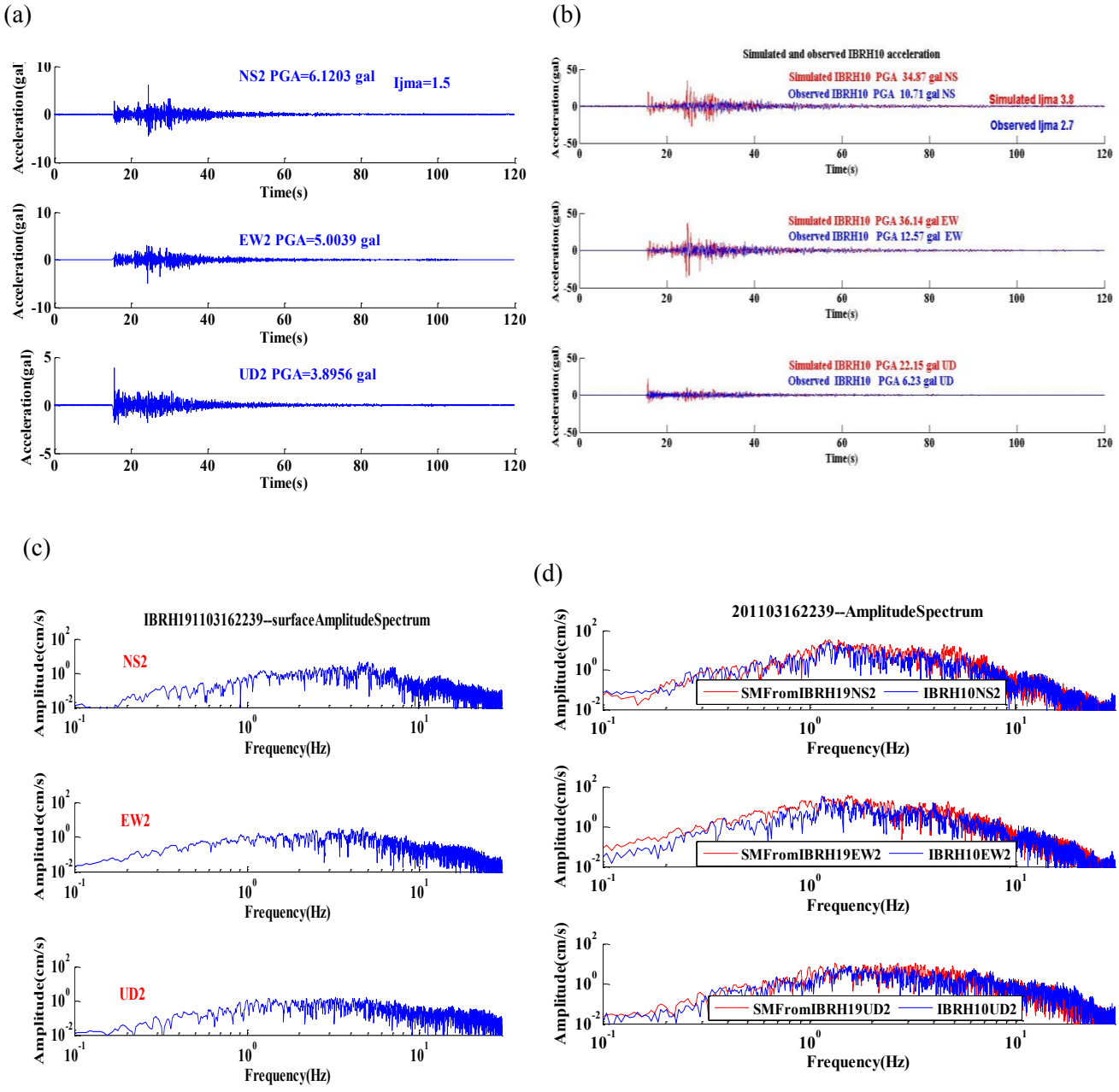

Figure 11. An example of simulation from IBRH19 (surface) to IBRH10 (surface) for the earthquake 201103162239: (a) the observed surface acceleration for IBRH19, (b) the observed surface acceleration waveform (blue) compared with the simulated one (red), (c) the spectral of observed surface record for IBRH19, (d) the observed spectra of surface record at IBRH10 (blue) compared with the simulated one (red)

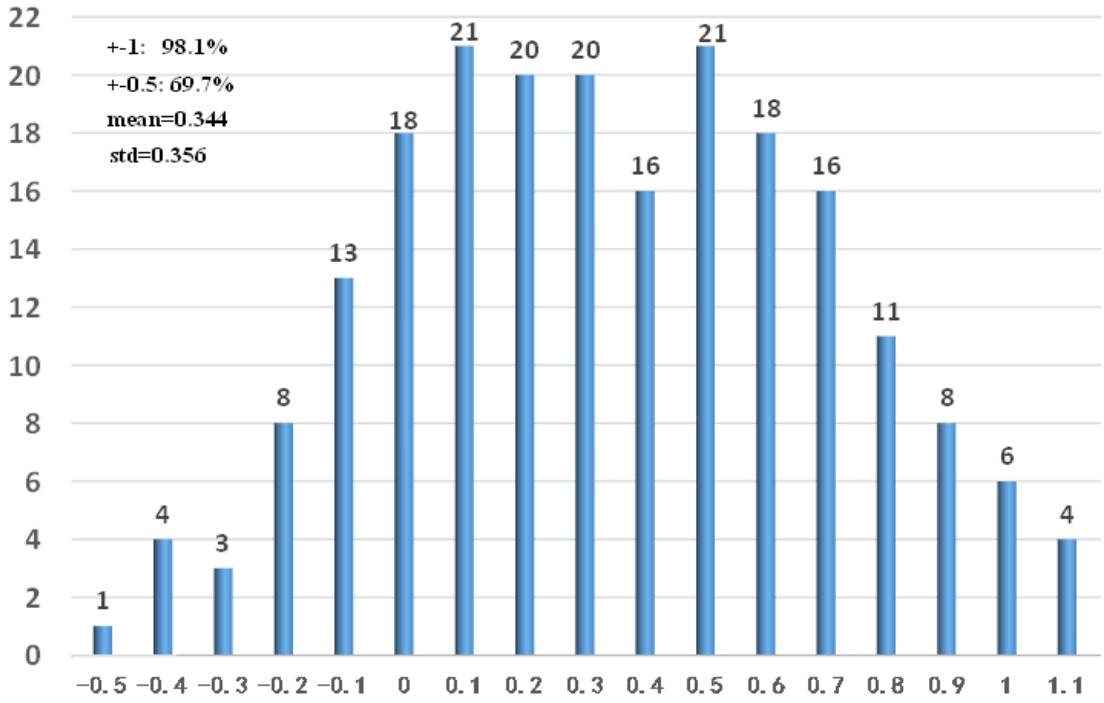

Figure 12. The seismic intensity residuals between the observed data and simulated data.

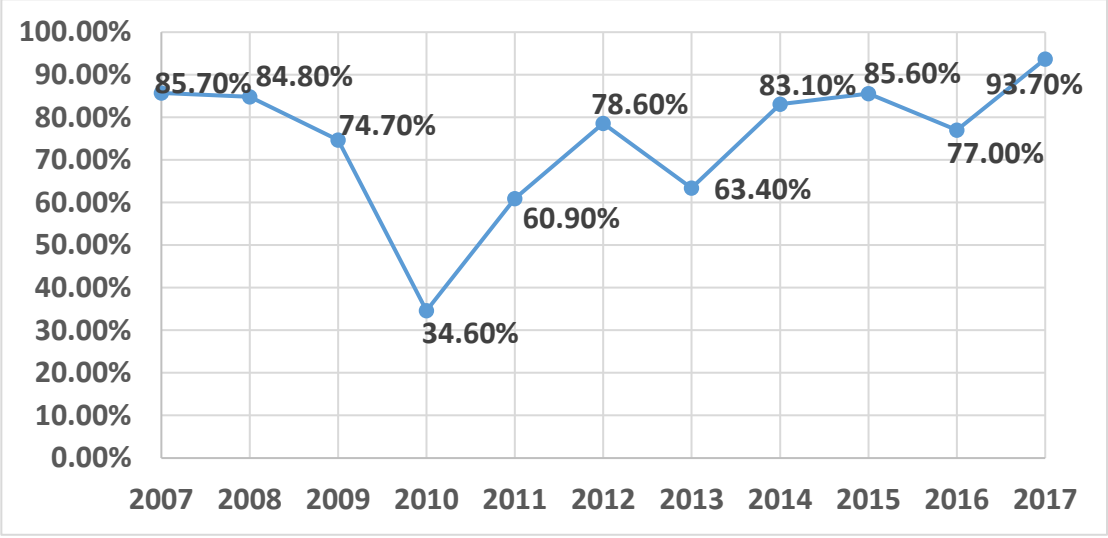

Figure 13. The percent ratio diagram for 1 degree seismic intensity error in the current Japan EEW System

5 Discussion

Through compare different simulation cases, it can be easily find that frequency-dependent correction of site amplification factor could produce different amplification factor for different earthquakes. It could produce the frequency-dependent site amplification factor. It highly improves the situation that scalar value site amplification methods which could not produce different amplification factor for different earthquakes. It skips the procedure to calculate the EEW magnitude and epicenter distance or hypocenter distance using the start potion of the waveform. We can obtain the waveform real-timely at the target station. It highly improve the accuracy of predicting ground motion real-timely compared with the scalar value site amplification factor. The simulation from borehole to surface is not suitable for earthquake early warning system. But it shows that this method shows good performance for real time simulating waveforms of the target station. Compare the two different simulation cases, it shows that the smaller distance between two stations, the seismic intensity prediction is more accurate. But for earthquake early warning purpose, we need to save much lead time for warning to the public that needs the distance between two stations much larger. It means that the method have relation with network density. We could use the frequency-dependent site implication factor to predict the seismic intensify more accurately in the seismic intensity quick report system with high network density. For earthquake early warning purpose, we need to use large amount of historical ground motion records to model the relative site amplification and search the optional casual filter parameter firstly. In the area with sparse network and low seismicity, we could not get the relative site amplification easily because of little amount of strong motion records. We need to consider other methods to estimate relative site amplification factor. We can adopt the method such as coda normalization method(Philips and Aki,196),generalized spectrum inversion method(Iwata and Irikura,1986;Kato et al.,1992) There are the cases that some simulation did not work very well.1.9% of the seismic intensity residuals is larger than 1.One of possible reason is azimuth dependency of site amplification(Cultrea et al.2002). We did not consider azimuth dependency in designing the frequency-dependent site amplification factor filter. If we design multiple frequency-dependent site amplification factor correction filter regarding the azimuth dependency of site amplification, we could be able to predict the target ground motion more precisely. Another possible reason is the accuracy of the input relative spectrum ratio, This situation may be improved by more precisely characterize the input spectral ratio and complicated filter design. For example, we can use a large number of first and second order filter to model the spectral ratio, but it is more complicated and time consuming for the hardware design when the number of filter grows larger. We need to make trade between the accuracy of the input spectral ratio and the difficulty of the filter design. This method pays attention to the amplitude characteristic and ignore the phase characteristic, there are few research on how to consider the phase in the earthquake early warning system. This situation may be improved the seismic interferometry method (Yamada et al. 2010). Because the site amplification factor was assumed as linear system, so the nonlinearity of weak ground motion and strong ground motion(Noguchi et al .2012) was not taken into consider in this study. More research are needed to solve these problems.

6 Conclusion

In this paper, we make full evaluation of the method that model the relative site amplification factor by historical strong ground motion data and then implementing the relative site amplification factor by the casual filter. First, we calculated the spectrum ratio for IBRH10 and IBRH19, then we got the surface simulated acceleration time series and spectrum for IBRH10 from borehole records at IBRH10. Similarly, we got the IBRH10 simulated surface acceleration time series and spectrum from the surface strong ground motion records of IBRH19.At last, we calculated the seismic intensity residual between the observed data and simulated data, and then compared the accuracy with the previous method and statistical report. This method highly improve the accuracy of predicting ground motion real-timely. The result shows as following:

(1) The spectra ratio is calculated between borehole record and surface record from the same station. Then we use infinite impulse recursive filter method to model our relative spectra ratio. The average seismic intensity residual of these earthquakes is 0.139. The standard deviation of these seismic intensity residuals is 0.254. 98.6% of these seismic intensity residuals is less than 0.5. 100% of these seismic intensity residuals is less than 1.

(2) The spectra ratio is calculated between IBRH10 and IBRH19 surface records. Similarly, we use infinite impulse recursive filter method to model the relative spectra ratio between two stations. The average seismic intensity residual of these earthquakes is 0.35. The standard deviation of these seismic intensity residuals is 0.36. 69.7% of these seismic intensity residuals is less than 0.5. 98.1% of these seismic intensity residuals is less than 1.This method shows better performance than the ARV method and station correction method. The average 1 degree seismic intensity error of all the eleven years statistical data of the current Japan Meteorological Agency earthquake early warning system is 74.74%. This method also shows better performance than the current operational Japan Meteorological Agency earthquake early warning system. This method highly improve the accuracy of predicting ground motion real-timely.

Data availability.

The hypocenter parameters including origin time, location of hypocenter, and magnitude used in this study, which were routinely determined by JMA, were obtained from the JMA seismic catalog. The KiK-net strong motion data can be downloaded from NIED website (http://www.kyoshin.bosai.go.jp/).Thanks to JMA and NIED for their hard work.

Author contributions.

XQ completed the core work and wrote the text content, QM and JZ were the technical director in chief, and HY supervised the strong motion data processing and related analysis. All authors discussed the editors' opinions and revised the paper.

Competing interests.

The authors declare that they have no conflict of interest.

Acknowledgements.

This work is partially supported by the Scientific Research Fund of Institute of Engineering Mechanics, China Earthquake Administration (Grant No.2016B02), National Natural Science Foundation of China (Grant No. 41874059).Thanks to Dr. Toshiaki Yokoi (BRI) and Dr. Mitsuyuki Hoshiba (MRI) for giving XQ supervision and useful suggestions for this study. And also thanks to Dr. Toshihide Kashima (BRI) for providing the program that used to calculate the JMA seismic intensity.

References

Alcik, H., Ozel, O., Apaydin, N., and Erdik, M.: A study on warning algorithms for Istanbul earthquake early warning system, Geophysical Research Letters 36, L00B05. 2009.

Allen, R. M., and Kanamori, H.: The potential for earthquake early warning in southern California, Science 300, 786–789, 2003.

Allen, R. M., Brown, H., Hellweg, M., Khainovski, O., Lombard, P., and Neuhauser, D.: Real-time earthquake detection and hazard assessment by ElarmS across California, Geophysical Research Letters 36, L00B08, 2009.

Bose, M., Hauksson, E., Solanki, K., Kanamori, H., and Heaton ,T. H.: Real-time testing of the on-site warning algorithm in southern California and its performance during the July 29, 2008Mw 5.4 Chino Hills earthquake, Geophysical Research Letters 36, L00B03, 2009.

Erdik, M., Fahjan, Y., Ozel, O., Alcik, H., Mert, A., and Gul, M.: Istanbul earthquake rapid response and the early warning system, Bulletin of Earthquake Engineering 1, 157–163, 2003.

Espinosa-Aranda, J. M., Cuellar, A., Garcia, A., Ibarrola, G., Islas, R., Maldonado, S. and Rodriguez, F. H.: Evolution of the MexicanSeismic Alert System (SASMEX), Seismological Research Letters 80(5), 694–706, 2009.

Espinosa-Aranda, J. M., Jimenez, A., Ibarrola, G., Alcantar, F., Aguilar, A., Inostroza, M., and Maldonado, S.: Mexico City Seismic Alert System, Seismological Research Letters 66, 42–52, 1995.

Horiuchi, S., Negishi, H., Abe, K., Kamimura, A., and Fujinawa, Y.: An automatic processing system for broadcasting earthquake alarms, Bulletin of the Seismological Society of America 95, 708–718, 2005.

Horiuchi, S., Horiuchi, Y., Yamamoto, S., Nakajima, H., Wu, C., Rydelek, P. A., and Kachi, M.: Home seismometer for earthquake early warning, Geophysical Research Letters 36, L00B04, 2009.

Hoshiba, M., Kamigaichi, O., Saito, M., Tsukada, S., and Hamada, N.: Earthquake early warning starts nationwide in Japan, Eos,Transactions, American Geophysical Union 89, 73–80, 2008.

Hoshiba, M., Iwakiri,K., Hayashimoto,N., Shimoyama,T., Hirano,K., Yamada,Y., Ishigaki,Y., and Kikuta,H.: Outline of the 2011 off the Pacific coast of Tohoku Earthquake (Mw 9.0), Earth Planets Space, 63, 547–551,2011.

Hoshiba, M.: Real Time Correction of Frequency-Dependetnt Site Amplification Factors for Application to Earthquake Early Warning, Bull.Seismo.Am.103 (6), 3179-3188,2013.

Hsiao, N. C., Wu, Y. M., Shin, T. C., Zhao, L., and Teng, T. L.: Development of earthquake early warning system in Taiwan, Geophysical Research Letters 36, L00B02, 2009.

Ionescu, C., Bose, M., Wenzel, F., Marmureanu, A., Grigore, A., and Marmureanu, G.: Early warning system for deep Vrancea (Romania) earthquakes, In Earthquake Early Warning Systems,ed. P. Gasparini, G., 2007.

Iwakiri,K., Hoshiba,M., Nakamura,K., Morikawa,N.: Improvement in the accuracy of expected seismic intensities for earthquake early warning in Japan using empirically estimated site amplification factors, Earth, Planets and Space.63, 57-69.

Iwata, T., and Irikura, K.: Source parameters of the 1983 earthquake sequence, J. Phys. Earth, 36, 155-184,1988.

Japan Meteorological Agency: The EEW statistical report on the Japan Meteorological Agency EEW system [EB/0L]. [Last accessed on 2018-11-20] http://www.data.jma.go.jp/svd/eqev/data/study-panel/eew-hyoka/10/shiryou1-1.pdf (in Japanese), 2018.

Kamigaichi, O.: JMA earthquake early warning, Journal of the Japan Association for Earthquake Engineering 4, 134–137, 2004.

Nakamura, H., Yamamoto, S., Horiuchi, S., Kunugi, T., Aoi, S., Fujiwara, H., and Ashiya, K.: Local Site Effects on the slope of the initial part of the P-wave envelope, Progeamme and Abstracts, the Seismological Society of Japan, 2006, Fall Meeting (in Japanese), 2006.

Nakamura, H., Horiuchi, S., Wu, C., Yamamoto, S., and Rydelek, P. A.: Evaluation of the real-time earthquake information system in Japan, Geophysical Research Letters 36, doi: 10.1029/2008GL036470, 2009.

Peng, H. S., Wu, Z. L., Wu, Y. M., Yu, S. M., Zhang, D. N., and Huang, W. H.: Developing a Prototype Earthquake Early Warning System in the Beijing Capital Region, Seismological Research Letters 81, 2011.

Wenzel, F., Onescu, M., Baur, M., and Fiedrich, F.: An early warning system for Bucharest, Seismological Research Letters 70, 161–169, 1999.

Wu, Y. M., Teng, T. L.: A virtual subnetwork approach to earthquake early warning, Bulletin of the Seismological Society of America 92, 2008–2018, 2002.

Yamada,M., Mori,J., and Ohmi,S.: Temporal changes of subsurface velocities during strong shaking as seen from seismic interferometry, Journal of Geophysical Research 115,B03302, 2010.

Yamazaki F, Noda S, Meguro K.: Developments of early earthquake damage assessment systems in Japan, Proc. of 7th International Conference on Structural Safety and Reliability, 1573-1580, 1998.

Zollo, A., Lancieri, M., and Nielsen, S.: Earthquake magnitude estimation from peak amplitudes of very early seismic signals on strong motion records, Geophysical Research Letters 33, L23312, 2006.

Zollo, A., Iannaccone, G., Lancieri, M., Cantore, L., Convertito, V., Emolo, A., Festa, G., Gallovic, F., Vassallo, M., Martino, C., Satriano, C., and Gasparini, P.: Earthquake early warning system in southern Italy: Methodologies and performance evaluation, Geophysical Research Letters 36, L00B07, 2009.

Iwata, T., and Irikura, K.: Separation of source, propagation and site effects from observed S-waves.,Zisin II, 39:579–593, 1986. (In Japanese with English abstract).

Phillips, W. S., Aki, K.: Site amplification of coda waves from local earthquakes in central California, Bulletin of the Seismological Society of America, 76:627-648, 1986.

Kato, K., Takemura, M., Ikeura, T., Urao, K., Uetake, T: Preliminary analysis for evaluation of local site effects from strong motion spectra by an inversion method,J. Phys. Earth, 40:175–191, 1992.

Cultrera, G., Rovelli, A., Mele, G., Azzara, R., Caserta, A., and Marra. F.: Azimuth-dependent amplification of weak and strong ground motions within a faultzone (Nocera Umbra, central Italy), Journal of Geophysical Research, 108, B3, DOI: 10.1029/2002JB001929, 2003.

Noguchi, S., Sato, H., and Sasatani, T: Characterization of nonlinear site response based on strong motion records at K-NET and KiK-net stations in the east of Japan., Proc. of 15th World Conference on Earthquake Engineering, Lisbon, Portugal, 24–28 September 2012, abstract number 3846.